

Supplemental Information 1 (SII)**Crystallographic preferred orientation of quartz (CPOs) methodology**

Complete crystallographic orientation data of quartz for were obtained using the Electron Back Scatter Diffraction (EBSD) technique and the following methodology.

Data were collected through an HKL EBSD detector installed on a JEOL JSM636OLV Scanning Electron Microscope (SEM) at Colgate University, located in Hamilton, New York, USA. Oxford Instruments HKL Channel 5.0 software was used for acquisition and processing of data. The following SEM conditions were used: high-vacuum mode, accelerating voltage of 20kV and a working distance of 12-20mm (optimal at 15-20mm). Samples were initially polished to a standard probe polish then subsequently polished on a vibrating table for 4-6 hours using a slightly basic solution to ensure both a mechanical and chemical final polish. Following this process, samples were mounted uncoated within the SEM.

EBSD analyses were collected using automated mapping where individual point data for quartz were measured at established intervals (step sizes) and automatically indexed to determine crystallographic orientations. Step sizes varied from 5 to 40 μm (typically 20 μm), and were set at increments smaller than the smallest grain size in a given sample to ensure sampling of all grains. The scanning area was variable (typically approximately 1cm² in total) and was increased in area until a minimum of 250 separate quartz grains were analyzed. (The method by which individual quartz grains and grain boundaries were distinguished is presented in the following paragraph).

Following data acquisition, wild data spikes were extrapolated and clusters of proximal point data with crystallographic misorientations less than 10° were grouped and filled in using a nearest-neighbor algorithm. This eliminated any erratic or misindexed crystallographic orientations. Following this, crystallographic misorientations greater than 10° were defined as grain boundaries; clusters of similar crystallographic orientations were classified as individual grains; and a new data set was created where each grain was represented as a single point. This eliminated any bias created by oversampling large grains, and provided results analogous to what could be derived from the traditional universal-stage (U-Stage) method.

An example of the data collection and processing is presented in figure SI1-A.

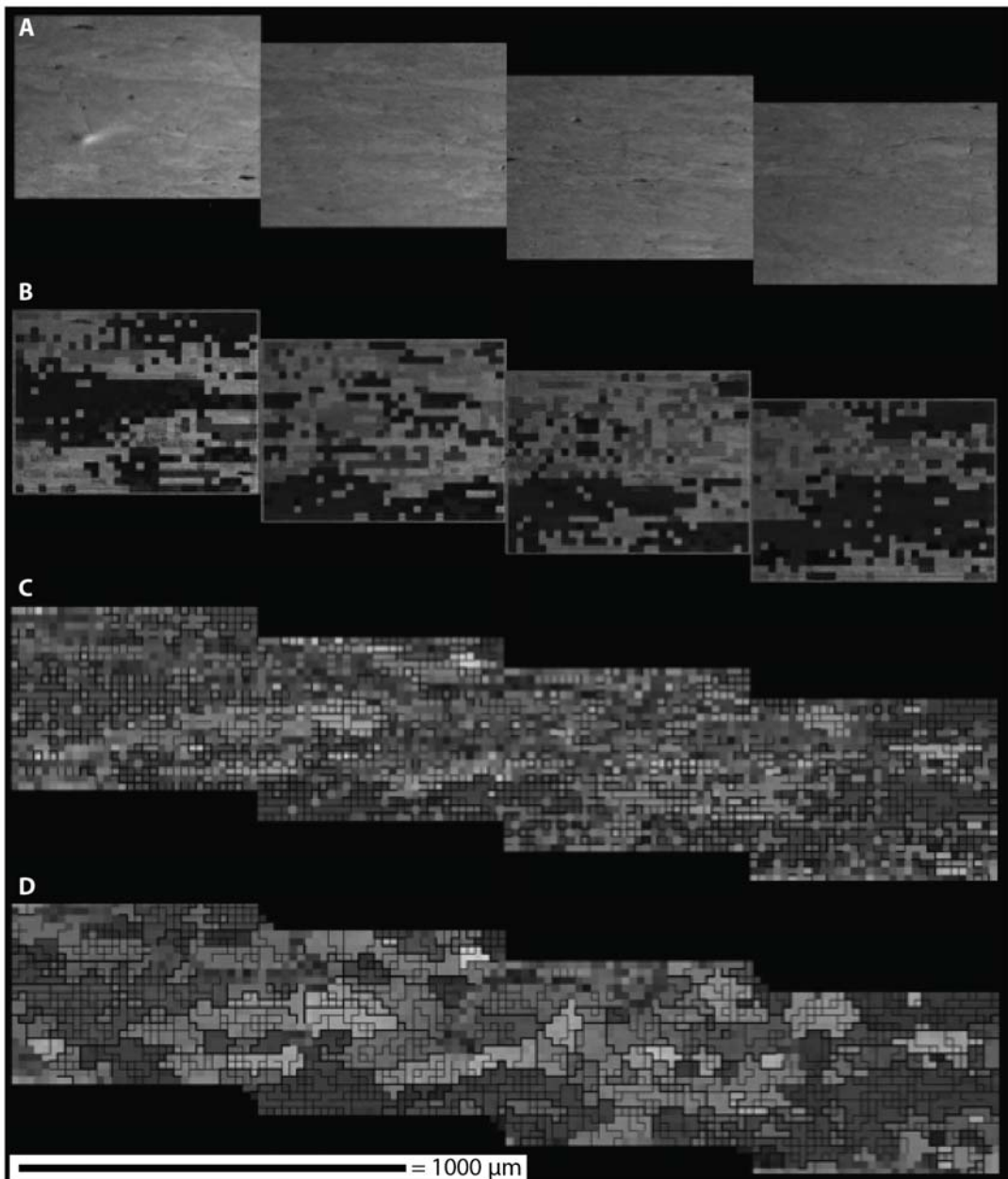


Figure SI1-A. Example of how CPOs were collected and processed using the EBSD method, for sample HK140. (A) SEM images of scanning areas from which data was collected. (B) Indexed quartz electron backscatter patterns overlain on SEM images. (C) Rasterized data image where different shades of grey represent different clusters of crystallographic orientations. (D) Post extrapolation of wild spikes and application of nearest neighbour algorithm. Using this modified data set, a new CPO data set was created whereby each grain (as seen by a set of pixels with the same shade of grey) was chosen to represent an individual point.

Supplemental Information 2 (SI2)

U-Th/Pb monazite geochronology methodology

U-Th/Pb geochronology was performed on monazite grains using the following methodology. Individual monazite grains were compositionally mapped for Th, Y, U and Nd / La using a JEOL JXA-8230 electron microprobe at Queen's University. This was completed to identify chemical zonation within the grains to facilitate targeting individual compositional domains. The following electron microprobe conditions were used: accelerating voltage of 15 kV, a beam current of ~350-500 nA, a dwell time of 100 ms and a step size of 0.5-1.2 μm . High- and low-magnification backscatter-electron and secondary-electron images were also collected to establish the textural context and physical condition of the monazite grains.

Monazites were analysed using a laser ablation multi collector inductively coupled plasma mass spectrometer (LA-MC-ICPMS) system housed at the University of California, Santa Barbara (UCSB). Instrumentation consists of a Nu Plasma MC-ICPMS (Nu Instruments, Wrexham, UK) and a 193 nm ArF laser ablation system equipped with a two-volume 'HelEx' ablation cell that facilitates rapid transfer and washout of ablated material (Photon Machines, San Diego, USA). Analytical protocol is similar to that described by Cottle et al. (2009a,b, 2011, 2012) with the modification that the collector arrangement on the Nu Plasma at UCSB allows for simultaneous determination of ^{232}Th and ^{238}U on high-mass side Faraday cups equipped with 10^{11} ohm resistors and ^{208}Pb , ^{207}Pb , ^{206}Pb and ^{204}Pb on four low-mass side ETP discrete dynode secondary electron multipliers.

U-Th/Pb analyses were conducted for 20 seconds each using a 7 μm spot diameter, a frequency of 4 Hz and 1.2 J/cm^2 fluence (equating to crater depths of approximately 5- 6 μm). A primary reference monazite, "44096" (424 Ma Pb/U ID-TIMS age, Aleinikoff et al., 2006) was employed to monitor and correct for mass bias as well as Pb/U and Pb/Th down-hole fractionation. To monitor data accuracy, two secondary reference monazites "FC-1" (55.7 Ma Pb/U ID-TIMS age, Horstwood et al., 2003), and "Managotry" monazite (554 Ma Pb/U ID-TIMS age, Paquette et al. 1994) were analyzed concurrently (once every 5 unknowns) and mass bias- and fractionation-corrected based on measured isotopic ratios of the primary reference monazite. During the analytical period, repeat analyses of FC-1 gave a weighted mean $^{206}\text{Pb}/^{238}\text{U}$ age of 56.5 ± 0.4 Ma, MSWD = 0.7, and a weighted mean $^{208}\text{Pb}/^{232}\text{Th}$ age of 54.0 ± 0.3 Ma,

MSWD = 0.8 (2σ) (n = 15). Repeat analyses of Managotry yield a weighted mean $^{206}\text{Pb}/^{238}\text{U}$ age of 553.5 ± 3.3 Ma, MSWD = 0.5, and a weighted mean $^{208}\text{Pb}/^{232}\text{Th}$ age of 557.8 ± 3.1 Ma, MSWD = 0.7 (2σ) (n = 15). Data reduction, including corrections for baseline, instrumental drift, mass bias, down-hole fractionation and uncorrected age calculations were carried out using Iolite version 2.1.2. Full details of the data reduction methodology can be found in Paton et al. (2010). All uncertainties are quoted at 2σ and include contributions from the external reproducibility of the primary reference material for the $^{207}\text{Pb}/^{206}\text{Pb}$, $^{206}\text{Pb}/^{238}\text{U}$ ratios and $^{208}\text{Pb}/^{232}\text{Th}$ ratios. Concordia diagrams were constructed using Isoplot 3.75 (Ludwig, 2012).

REFERENCES

- Aleinikoff, J.N., Schenck, W.S., Plank, M.O., Srogi, L., Fanning, C.M., Kamo, S.L., and Bosbyshell, H., 2006, Deciphering igneous and metamorphic events in high-grade rocks of the Wilmington Complex, Delaware: Morphology, cathodoluminescence and backscattered electron zoning, and SHRIMP U-Pb geochronology of zircon and monazite: Geological Society of America Bulletin, v. 118, p. 39–64.
- Cottle, J. M., Searle, M. P., Horstwood, M. S. A., and Waters, D., 2009a, Timing of midcrustal metamorphism, melting, and deformation in the Mount Everest region of southern Tibet revealed by U(-Th)-Pb geochronology: Journal of Geology, v. 117, p. 643–664, doi:10.1086/605994.
- Cottle, J. M., Jessup, M. J., Newell, D. L., Horstwood, M.S. A., Noble, S. R., Parrish, R. R., Waters, D. J., and Searle, M. P., 2009b, Geochronology of granulitized eclogites from the Ama Drime Massif, implications for the tectonic evolution of the South Tibetan Himalaya: Tectonics, v. 28, p. TC1002, doi:10.1029/2008TC002256.
- Cottle, J.M., Waters, D.J., Riley, D., Beyssac, O., and Jessup, M.J., 2011, Metamorphic history of the South Tibetan detachment system, Mt. Everest region, revealed by RSCM thermometry and phase equilibria modeling: Journal of Metamorphic Geology, v. 29, p. 561– 582, doi:10.1111/j.1525-1314.2011.00930.x.
- Cottle, J.M., Kylander-Clark, A.R., Vrijmoed, J.C., 2012, U-Th/Pb geochronology of detrital zircon and monazite by single shot laser ablation inductively coupled mass spectrometry (SS-LA-ICPMS): Chemical Geology, v. 332-333, p. 136–147, doi:10.1016/j.chemgeo.2012.09.035.
- Horstwood, M.S.A., Foster, G.L., Parrish, R.R., Noble, S.R., and Nowell, G.M., 2003, Common-Pb corrected in situ U-Pb accessory mineral geochronology by LA-MC-ICPMS: Journal of Analytical Atomic Spectrometry, v. 18, p. 837–846.
- Ludwig, K. 2012, User's manual for Isoplot v.3.75: a geochronological toolkit for Microsoft Excel, Berkeley, CA: Berkely Geochronology Center Special Publication, v. 5: revised January 30, 2012, 75p.
- Paton, C., Woodhead, J., Hellstrom, J., Hergt, J., Greig, A., and Maas, R., 2010, Improved laser ablation U–Pb zircon geochronology through robust downhole fractionation correction: Geochemistry, Geophysics and Geosystems, v. 11, p. Q0AA06, doi:10.1029/2009GC002618.
- Paquette, J.L., Nédélec, A., Moine, B., and Rakotondrazafy, M., 1994, U-Pb, single zircon Pb-evaporation, and Sm-Nd isotopic study of a granulite domain in SE Madagascar: The Journal of Geology, v. 102, p. 523–538.

Supplemental Information 3 (SI3): U-Th/Pb geochronologic data table

Analysis	Position	Pb	U	Th	Th/U	$^{207}\text{Pb}/^{206}\text{Pb}$	2σ	$^{206}\text{Pb}/^{238}\text{U}$	2σ	$^{207}\text{Pb}/^{235}\text{U}^b$	2σ	Rho ^c	$^{208}\text{Pb}/^{232}\text{Th}$	2σ	$^{206}\text{Pb}/^{238}\text{U}$	2σ	$^{208}\text{Pb}/^{232}\text{Th}$	2σ
		(ppm) ^a	(ppm) ^a	(ppm) ^a			(%)		(%)		(%)		(%)	(%)	(Ma) ^d	abs	(Ma) ^e	abs
<u>KH18a</u>																		
HK18a_2_02	H-Y,R	59	4860	51700	10.4	0.0929	2.80	0.0027	1.96	0.0345	3.19	0.38	0.000817	2.08	17.4	0.3	16.5	0.3
HK18a_2_03	H-Y,R	66	6390	55700	8.4	0.0864	1.85	0.0028	2.00	0.033	2.61	0.74	0.000856	1.87	18.0	0.4	17.3	0.3
HK18a_2_04	H-Y,R	62	5180	54000	10.0	0.0878	1.94	0.0027	2.11	0.03311	2.84	0.72	0.000831	2.05	17.4	0.4	16.8	0.3
HK18a_2_05	H-Y,R	64	5590	54200	9.4	0.0844	2.13	0.00277	1.77	0.03223	2.79	0.66	0.000854	1.87	17.9	0.3	17.3	0.3
HK18a_2_06	H-Y,R	67	6510	56600	8.4	0.0852	1.88	0.00272	2.06	0.03165	2.91	0.73	0.000854	2.22	17.5	0.4	17.3	0.4
HK18a_2_07	H-Y,R	87	11200	67800	5.9	0.0848	1.13	0.00291	1.99	0.03391	2.12	0.84	0.000921	2.06	18.7	0.4	18.6	0.4
HK18a_2_08	H-Y,R	63	6910	48100	6.9	0.092	1.74	0.00303	1.98	0.0381	2.89	0.73	0.000938	2.13	19.5	0.4	19.0	0.4
HK18a_2_09	H-Y,R	71	7090	58700	8.2	0.0916	1.75	0.00282	2.17	0.03605	2.75	0.70	0.00086	2.21	18.1	0.4	17.4	0.4
HK18a_2_10	H-Y,R	72	7260	54800	7.6	0.1259	1.59	0.00305	1.87	0.0527	2.28	0.73	0.000929	1.94	19.7	0.4	18.8	0.4
HK18a_2_11	L-Y,C	84	13970	64200	4.8	0.0854	1.29	0.00292	1.82	0.03367	2.11	0.77	0.000921	1.95	18.8	0.3	18.6	0.4
HK18a_2_12	L-Y,C	91	13820	67700	5.2	0.1049	1.14	0.00301	2.36	0.0433	2.54	0.87	0.00095	2.32	19.4	0.5	19.2	0.4
HK18a_2_13	L-Y,C	92	10120	70700	7.6	0.0998	1.70	0.00304	2.30	0.041	2.68	0.81	0.000927	2.16	19.6	0.5	18.7	0.4
HK18a_2_14	L-Y,C	85	13290	62400	5.2	0.1167	1.20	0.00302	2.15	0.0487	2.46	0.88	0.000948	2.11	19.5	0.4	19.2	0.4
HK18a_2_15	L-Y,C	82	11810	60200	5.7	0.1185	1.43	0.00308	1.92	0.0498	2.01	0.78	0.00096	1.98	19.8	0.4	19.4	0.4
HK18a_2_16	L-Y,C	66	9500	50100	5.8	0.0937	1.49	0.00299	2.41	0.0383	2.87	0.82	0.000939	2.56	19.2	0.5	19.0	0.5
HK18a_2_17	H-Y,R	103	16470	74500	5.0	0.1459	4.46	0.00311	2.16	0.0642	5.92	0.69	0.000977	2.05	20.0	0.4	19.7	0.4
HK18a_2_18	H-Y,R	59	8230	47100	6.3	0.1182	3.98	0.00287	2.16	0.0471	5.10	0.64	0.000875	2.29	18.5	0.4	17.7	0.4
HK18a_2_19	L-Y,C	58	8490	44300	5.7	0.1082	2.59	0.00296	1.93	0.0443	3.16	0.62	0.00091	2.09	19.0	0.4	18.4	0.4
HK18a_4_01	L-Y,R	68	5480	39000	7.4	0.3788	1.06	0.00438	1.49	0.2274	2.11	0.85	0.001253	1.44	28.2	0.4	25.3	0.4
HK18a_4_11	L-Y,R	59	10410	45410	4.3	0.0825	1.21	0.00286	1.72	0.03323	2.29	0.83	0.000943	1.59	18.4	0.3	19.1	0.3
HK18a_5_03	Mix	90	9540	71900	7.9	0.1599	2.06	0.00296	1.76	0.0658	2.89	0.68	0.000911	1.87	19.1	0.3	18.4	0.3
HK18a_5_04	Mix	86	9730	61600	6.7	0.1717	3.38	0.0032	2.00	0.0763	4.59	0.77	0.001009	2.08	20.6	0.4	20.4	0.4
HK18a_5_05	Mix	136	12930	85700	7.0	0.3046	1.84	0.00402	2.11	0.1703	3.23	0.86	0.001156	2.08	25.9	0.6	23.4	0.5
HK18a_5_06	Mix	80	9230	56700	6.6	0.2168	2.91	0.00334	2.07	0.1005	4.18	0.82	0.00102	1.96	21.5	0.4	20.6	0.4
HK18a_5_07	Mix	78	10020	62600	6.6	0.0886	2.26	0.0028	1.72	0.0346	2.89	0.65	0.000898	1.67	18.0	0.3	18.1	0.3
HK18a_5_09	Mix	84	9670	61780	6.6	0.1323	2.72	0.00309	1.78	0.0564	3.19	0.66	0.000985	1.83	19.9	0.4	19.9	0.4
HK18a_5_10	Mix	79	9610	60100	6.4	0.1926	2.75	0.0031	2.19	0.0817	4.04	0.75	0.000949	2.00	20.0	0.4	19.2	0.4
HK18a_6_01	H-Y,R	69	8750	60700	6.9	0.0877	2.39	0.00265	1.73	0.03195	2.97	0.62	0.000821	1.83	17.1	0.3	16.6	0.3
HK18a_6_02	H-Y,R	69	9730	55900	5.7	0.0782	2.05	0.00276	1.63	0.03022	2.78	0.59	0.000884	1.70	17.8	0.3	17.9	0.3
HK18a_6_03	H-Y,R	90	9960	72000	7.1	0.088	1.82	0.00287	1.74	0.0352	3.13	0.70	0.00089	1.69	18.5	0.3	18.0	0.3
HK18a_6_04	H-Y,R	69	9300	55600	5.9	0.0793	2.14	0.00274	1.94	0.03011	2.99	0.64	0.000877	1.94	17.6	0.3	17.7	0.3
HK18a_6_05	H-Y,R	63	8290	51700	6.1	0.0775	2.32	0.00273	1.69	0.02906	2.99	0.61	0.000867	1.61	17.6	0.3	17.5	0.3
HK18a_6_06	H-Y,R	63	8280	56600	6.8	0.0781	2.43	0.00251	1.71	0.02727	2.97	0.54	0.000794	1.64	16.2	0.3	16.0	0.3
HK18a_6_08	H-Y,R	79	7160	48100	6.7	0.293	2.66	0.00379	2.01	0.153	4.12	0.88	0.001167	2.06	24.4	0.5	23.6	0.5
HK18a_6_09	H-Y,R	61	7540	49300	6.5	0.0773	1.55	0.00275	1.78	0.02959	2.84	0.79	0.000876	1.83	17.7	0.3	17.7	0.3

Analysis	Position	Pb	U	Th	Th/U	$^{207}\text{Pb}/^{206}\text{Pb}$	2σ	$^{206}\text{Pb}/^{238}\text{U}$	2σ	$^{207}\text{Pb}/^{235}\text{U}^b$	2σ	Rho ^c	$^{208}\text{Pb}/^{232}\text{Th}$	2σ	$^{206}\text{Pb}/^{238}\text{U}$	2σ	$^{208}\text{Pb}/^{232}\text{Th}$	2σ
		(ppm) ^a	(ppm) ^a	(ppm) ^a		(%)			(%)		(%)		(%)	(%)	(Ma) ^d	abs	(Ma) ^e	abs
HK18a_6_10	H-Y,R	64	7850	50400	6.4	0.0788	1.90	0.0028	1.61	0.03056	2.59	0.63	0.000898	1.78	18.0	0.3	18.2	0.3
HK18a_6_11	L-Y,C	54	7260	45420	6.3	0.0762	2.36	0.0026	2.11	0.02697	3.23	0.69	0.000831	2.17	16.8	0.4	16.8	0.4
HK18a_6_12	L-Y,C	48	6850	40030	5.8	0.1417	4.23	0.00263	1.97	0.0508	4.92	0.55	0.000849	2.12	17.0	0.3	17.2	0.4
HK18a_6_14	H-Y,R	71	6720	55500	8.3	0.1282	2.57	0.00293	1.95	0.0518	3.09	0.62	0.000895	1.79	18.9	0.4	18.1	0.3
HK18a_6_15	H-Y,R	66	6400	49500	7.8	0.0856	2.34	0.00296	1.72	0.035	3.14	0.62	0.000945	1.59	19.1	0.3	19.1	0.3
HK18a_7_02	H-Y,R	53	5760	47100	8.3	0.0932	1.82	0.00255	1.69	0.03317	2.80	0.71	0.000792	1.64	16.4	0.3	16.0	0.3
HK18a_7_03	H-Y,R	53	5056	43900	8.8	0.1357	2.21	0.00284	1.73	0.0528	3.03	0.63	0.000861	1.63	18.3	0.3	17.4	0.3
HK18a_7_04	H-Y,R	57	5940	47700	8.1	0.1035	1.93	0.00272	1.98	0.0387	2.84	0.69	0.000844	2.01	17.5	0.4	17.1	0.3
HK18a_7_05	L-Y,C	65	6490	49000	7.6	0.1034	1.64	0.00303	1.91	0.04259	2.30	0.69	0.00096	1.88	19.5	0.4	19.4	0.4
HK18a_7_06	L-Y,C	76	7130	55600	7.8	0.141	1.49	0.00313	1.92	0.0601	2.66	0.81	0.000976	1.95	20.1	0.4	19.7	0.4
HK18a_7_07	H-Y,R	70	6390	50000	7.9	0.1674	2.09	0.00326	1.66	0.0751	2.93	0.75	0.001006	1.69	21.0	0.4	20.3	0.4
HK18a_7_08	H-Y,R	71	6280	45590	7.3	0.2647	2.68	0.0036	2.03	0.1299	4.39	0.86	0.001113	1.98	23.2	0.5	22.5	0.4
HK18a_7_09	H-Y,R	71	6140	48000	7.8	0.2285	0.83	0.00349	1.43	0.1101	1.91	0.89	0.001063	1.41	22.5	0.3	21.5	0.3
HK18a_7_11	H-Y,R	96	8730	76200	8.6	0.0902	1.22	0.00294	1.87	0.03651	2.14	0.83	0.000896	1.90	18.9	0.4	18.1	0.3
HK18a_7_12	H-Y,R	86	8500	54000	6.3	0.2558	2.78	0.00374	2.08	0.1317	4.40	0.87	0.001152	1.91	24.1	0.5	23.3	0.5
HK18a_7_13	H-Y,R	58	5450	34300	6.2	0.3861	1.74	0.00398	2.36	0.2127	3.67	0.89	0.001195	2.18	25.6	0.6	24.1	0.5
HK18a_7_15	H-Y,R	82	8050	49110	6.1	0.3657	1.86	0.00406	1.99	0.2043	3.28	0.91	0.001175	1.96	26.1	0.5	23.7	0.5
HK18a_8_01	L-Y	100	8580	55700	6.6	0.4096	1.05	0.00472	1.78	0.2662	2.40	0.92	0.001267	1.74	30.4	0.5	25.6	0.4
HK18a_8_02	L-Y	78	10520	58600	5.8	0.1334	3.37	0.00303	1.91	0.0556	4.32	0.71	0.000941	1.91	19.5	0.4	19.0	0.4
HK18a_8_04	L-Y	108	13340	83300	6.3	0.0993	1.31	0.00295	1.80	0.04022	2.21	0.78	0.000916	1.86	19.0	0.3	18.5	0.3
HK18a_8_05	L-Y	76	6350	41800	6.7	0.3438	1.05	0.00423	1.73	0.1998	2.10	0.89	0.001272	1.81	27.2	0.5	25.7	0.5
HK18a_8_06	L-Y	133	13730	95500	7.0	0.149	1.88	0.00321	1.65	0.0661	2.57	0.73	0.00098	1.63	20.7	0.3	19.8	0.3
HK18a_8_09	H-Y	68	4404	57600	13.0	0.1058	2.84	0.00278	1.94	0.0407	3.69	0.63	0.000836	1.79	17.9	0.4	16.9	0.3
HK18a_8_10	H-Y	127	10540	86100	8.2	0.2044	4.84	0.00347	1.90	0.0987	6.28	0.82	0.00104	1.83	22.4	0.4	21.0	0.4
HK18a_8_11	H-Y	69	6190	56700	9.2	0.0836	2.15	0.00277	1.66	0.03174	2.65	0.61	0.000874	1.72	17.8	0.3	17.7	0.3
HK18a_8_12	H-Y	67	5520	52500	9.5	0.139	1.65	0.00298	2.05	0.0577	2.77	0.75	0.000919	1.96	19.2	0.4	18.6	0.4
HK18a_8_13	H-Y	86	5120	49400	9.6	0.3432	2.16	0.00442	1.99	0.2076	3.61	0.89	0.001261	1.90	28.4	0.6	25.5	0.5
HK18a_8_18	H-Y	73	5810	57500	9.9	0.1332	3.75	0.00297	1.65	0.0545	4.77	0.71	0.000915	1.64	19.1	0.3	18.5	0.3
HK18a_8_19	H-Y	115	10410	89400	8.6	0.0909	1.21	0.00296	1.83	0.03699	2.27	0.80	0.000921	1.63	19.0	0.4	18.6	0.3
HK18a_8_20	H-Y	62	4690	53500	11.4	0.0944	1.69	0.00272	2.02	0.03555	2.62	0.73	0.000838	2.03	17.5	0.4	16.9	0.3
<u>HK109</u>																		
HK109_2_01	H-Y,R	36	5867	34488	5.88	0.08409	2.97	0.00236	2.16	0.02710	3.46	0.57	0.000708	2.42	15.2	0.3	14.3	0.3
HK109_2_02	H-Y,R	39	6970	36542	5.25	0.08084	2.61	0.00242	2.44	0.02719	3.48	0.73	0.000746	2.43	15.6	0.4	15.1	0.4
HK109_2_03	H-Y,R	42	7859	38601	4.93	0.07828	2.82	0.00246	1.98	0.02649	2.92	0.48	0.000759	2.13	15.8	0.3	15.3	0.3
HK109_2_04	H-Y,R	41	7076	39225	5.61	0.08228	3.05	0.00243	2.29	0.02746	3.64	0.59	0.000740	2.47	15.7	0.4	14.9	0.4
HK109_2_05	H-Y,R	45	7227	41952	5.77	0.07755	2.74	0.00248	2.52	0.02657	3.50	0.60	0.000751	2.73	16.0	0.4	15.2	0.4
HK109_2_06	H-Y,R	49	8150	48583	6.02	0.08200	3.39	0.00234	2.60	0.02683	4.70	0.70	0.000713	2.66	15.1	0.4	14.4	0.4
HK109_2_07	H-Y,R	52	10055	49174	4.93	0.07728	2.81	0.00245	2.54	0.02589	3.51	0.65	0.000760	2.53	15.8	0.4	15.4	0.4
HK109_2_08	H-Y,R	38	6694	40851	6.15	0.09938	3.50	0.00219	2.47	0.02943	3.96	0.55	0.000665	2.13	14.1	0.3	13.4	0.3

Analysis	Position	Pb	U	Th	Th/U	$^{207}\text{Pb}/^{206}\text{Pb}$	2σ	$^{206}\text{Pb}/^{238}\text{U}$	2σ	$^{207}\text{Pb}/^{235}\text{U}^b$	2σ	Rho ^c	$^{208}\text{Pb}/^{232}\text{Th}$	2σ	$^{206}\text{Pb}/^{238}\text{U}$	2σ	$^{208}\text{Pb}/^{232}\text{Th}$	2σ
		(ppm) ^a	(ppm) ^a	(ppm) ^a		(%)			(%)		(%)		(%)	(%)	(Ma) ^d	abs	(Ma) ^e	abs
HK109_2_09	L-Y,C	77	9813	62883	6.46	0.08099	2.31	0.00280	2.48	0.03128	3.21	0.73	0.000869	2.52	18.0	0.4	17.5	0.4
HK109_2_10	L-Y,C	81	10218	65197	6.37	0.08466	1.92	0.00285	2.58	0.03316	3.34	0.82	0.000884	2.59	18.4	0.5	17.9	0.5
HK109_2_11	L-Y,C	78	9474	64086	6.76	0.08304	2.22	0.00283	2.45	0.03245	3.29	0.74	0.000864	2.50	18.2	0.4	17.4	0.4
HK109_3_01	L-Y	69	11710	61451	5.19	0.07357	2.81	0.00261	2.51	0.02678	4.09	0.80	0.000803	2.78	16.8	0.4	16.2	0.4
HK109_3_02	L-Y	68	11470	60350	5.20	0.07432	2.66	0.00266	3.16	0.02705	3.69	0.72	0.000814	3.46	17.1	0.5	16.4	0.6
HK109_3_03	L-Y	67	11405	59740	5.25	0.07489	2.21	0.00264	2.79	0.02698	3.41	0.75	0.000803	2.67	17.0	0.5	16.2	0.4
HK109_3_04	L-Y	67	11379	59548	5.20	0.07386	2.11	0.00266	3.50	0.02729	4.24	0.88	0.000821	3.46	17.1	0.6	16.6	0.6
HK109_3_05	L-Y	75	11210	62640	5.58	0.07935	2.30	0.00277	3.27	0.03015	4.08	0.80	0.000858	3.39	17.8	0.6	17.3	0.6
HK109_3_06	L-Y	87	12143	72044	5.90	0.08758	2.20	0.00284	3.29	0.03445	3.90	0.82	0.000869	3.12	18.3	0.6	17.6	0.5
HK109_4_01	H-Y,R	39	6869	39827	5.73	0.13569	4.58	0.00234	2.86	0.04434	5.86	0.63	0.000722	3.05	15.1	0.4	14.6	0.4
HK109_4_03	H-Y,R	46	9983	50358	4.96	0.09315	4.04	0.00207	2.72	0.02679	4.99	0.62	0.000662	2.75	13.3	0.4	13.4	0.4
HK109_4_04	H-Y,R	54	9944	57213	5.75	0.08418	2.63	0.00225	2.72	0.02632	3.46	0.69	0.000669	2.64	14.5	0.4	13.5	0.4
HK109_4_05	H-Y,R	57	13529	60859	4.48	0.07607	2.36	0.00222	3.16	0.02308	3.84	0.83	0.000673	3.35	14.3	0.5	13.6	0.5
HK109_4_06	L-Y,C	70	9381	60399	6.43	0.07447	2.79	0.00266	3.08	0.02758	4.04	0.73	0.000817	2.93	17.2	0.5	16.5	0.5
HK109_4_07	L-Y,C	68	8584	58399	6.85	0.07471	2.25	0.00266	2.56	0.02737	3.15	0.78	0.000818	2.70	17.1	0.4	16.5	0.4
HK109_4_08	L-Y,C	67	7730	57545	7.41	0.07607	2.36	0.00271	2.75	0.02868	3.42	0.74	0.000839	2.73	17.5	0.5	17.0	0.5
HK109_4_09	L-Y,C	60	7446	52272	7.08	0.07421	2.40	0.00267	3.03	0.02731	3.66	0.75	0.000812	2.80	17.2	0.5	16.4	0.5
HK109_4_10	H-Y,R	63	7041	52058	7.62	0.07419	2.22	0.00279	2.53	0.02860	3.16	0.71	0.000853	2.56	17.9	0.5	17.2	0.4
HK109_5_01	H-Y,R	40	5150	40823	8.15	0.08141	3.37	0.00230	3.21	0.02605	4.68	0.71	0.000695	2.99	14.8	0.5	14.0	0.4
HK109_5_02	H-Y,R	40	5334	40577	7.78	0.08141	3.04	0.00232	3.06	0.02622	4.05	0.68	0.000710	3.16	14.9	0.5	14.3	0.5
HK109_5_04	H-Y,R	43	6121	43391	7.18	0.08018	3.26	0.00237	4.04	0.02610	5.10	0.79	0.000719	4.00	15.3	0.6	14.5	0.6
HK109_5_05	H-Y,R	43	6068	43384	7.20	0.07952	3.42	0.00232	3.25	0.02551	4.65	0.69	0.000702	3.39	15.0	0.5	14.2	0.5
HK109_5_06	L-Y	136	7741	53854	6.85	0.06516	1.70	0.00599	3.64	0.05342	3.86	0.91	0.001823	3.52	38.5	1.4	36.8	1.3
HK109_5_07	L-Y	66	7660	51408	6.64	0.07722	2.60	0.00281	3.53	0.02971	4.17	0.82	0.000907	3.39	18.1	0.6	18.3	0.6
HK109_5_08	H-Y,R	58	7943	51836	6.50	0.07634	2.71	0.00252	3.93	0.02652	4.96	0.84	0.000787	3.89	16.2	0.6	15.9	0.6
HK109_5_09	H-Y,R	348	5671	40765	7.14	0.06162	1.30	0.01554	4.58	0.13254	4.67	0.95	0.006171	4.46	99.4	4.5	124.3	5.5
HK109_5_10	M-Y,C	622	3261	23161	6.95	0.05881	0.98	0.06527	3.66	0.52320	3.45	0.96	0.019476	4.11	407.2	##	389.7	##
HK109_6_01	H-Y,R	53	7831	50546	6.69	0.07684	2.81	0.00237	3.82	0.02574	4.36	0.80	0.000722	3.52	15.3	0.6	14.6	0.5
HK109_6_02	H-Y,R	55	8356	53705	6.66	0.07975	2.66	0.00239	3.72	0.02638	4.14	0.82	0.000738	3.55	15.4	0.6	14.9	0.5
HK109_6_03	H-Y,R	58	8768	55526	6.64	0.07890	2.45	0.00242	3.70	0.02603	4.04	0.85	0.000737	3.54	15.6	0.6	14.9	0.5
HK109_6_04	H-Y,R	56	8435	54456	6.84	0.08103	3.02	0.00240	4.10	0.02682	4.89	0.79	0.000725	4.06	15.5	0.6	14.7	0.6
HK109_6_05	H-Y,R	64	10273	59909	6.24	0.07919	2.73	0.00250	3.46	0.02779	4.28	0.79	0.000771	3.34	16.1	0.6	15.6	0.5
HK109_6_06	L-Y,C	69	16150	61746	4.09	0.07015	2.16	0.00258	3.04	0.02433	4.01	0.84	0.000813	3.19	16.6	0.5	16.4	0.5
HK109_6_07	L-Y,C	70	15297	61477	4.29	0.06847	2.35	0.00256	3.43	0.02408	4.05	0.83	0.000805	3.31	16.5	0.6	16.3	0.5
HK109_6_08	H-Y,R	58	9043	56834	6.67	0.08013	2.36	0.00240	3.62	0.02593	4.35	0.86	0.000745	3.67	15.4	0.6	15.1	0.6
HK109_6_09	H-Y,R	62	9204	58088	6.70	0.08204	2.43	0.00248	3.29	0.02828	4.39	0.82	0.000763	3.32	16.0	0.5	15.4	0.5
HK109_6_10	H-Y,R	50	7279	49743	7.07	0.08405	2.77	0.00236	3.31	0.02716	3.95	0.73	0.000731	3.55	15.2	0.5	14.8	0.5
HK109_9_01	H-Y,R	56	8315	53777	6.47	0.08691	4.39	0.00244	3.84	0.02973	6.04	0.63	0.000740	3.99	15.7	0.6	15.0	0.6
HK109_9_02	H-Y,R	53	7283	51789	7.07	0.08960	2.59	0.00246	3.94	0.03029	4.45	0.79	0.000738	3.61	15.8	0.6	14.9	0.5
HK109_9_03	H-Y,R	67	11173	57095	4.96	0.07526	2.72	0.00274	5.22	0.02873	5.50	0.86	0.000857	5.04	17.7	0.9	17.3	0.9

Analysis	Position	Pb	U	Th	Th/U	$^{207}\text{Pb}/^{206}\text{Pb}$	2σ	$^{206}\text{Pb}/^{238}\text{U}$	2σ	$^{207}\text{Pb}/^{235}\text{U}^b$	2σ	Rho ^c	$^{208}\text{Pb}/^{232}\text{Th}$	2σ	$^{206}\text{Pb}/^{238}\text{U}$	2σ	$^{208}\text{Pb}/^{232}\text{Th}$	2σ
		(ppm) ^a	(ppm) ^a	(ppm) ^a		(%)			(%)		(%)		(%)	(%)	(Ma) ^d	abs	(Ma) ^e	abs
HK109_9_04	L-Y,C	69	10626	58723	5.47	0.08263	2.43	0.00276	4.20	0.03147	5.29	0.87	0.000843	4.28	17.8	0.7	17.0	0.7
HK109_9_05	L-Y,C	56	8767	44249	5.00	0.08638	2.33	0.00294	4.16	0.03449	4.49	0.84	0.000926	4.24	18.9	0.8	18.7	0.8
HK109_9_06	L-Y,C	62	9834	51784	5.24	0.08787	2.26	0.00277	3.37	0.03311	3.89	0.79	0.000855	3.60	17.8	0.6	17.3	0.6
HK109_10_01	L-Y	80	14739	71543	4.71	0.07048	2.74	0.00259	3.04	0.02484	4.16	0.77	0.000813	2.87	16.7	0.5	16.4	0.5
HK109_10_02	H-Y	77	8491	63171	7.28	0.08345	2.49	0.00291	3.72	0.03354	4.21	0.82	0.000882	3.67	18.8	0.7	17.8	0.7
HK109_10_03	H-Y	66	8296	54042	6.40	0.07404	3.00	0.00289	3.55	0.02939	4.51	0.76	0.000900	3.68	18.6	0.7	18.2	0.7
HK109_10_04	H-Y	65	7777	54415	6.79	0.07879	2.94	0.00284	4.53	0.03091	5.10	0.82	0.000886	4.36	18.4	0.8	17.9	0.8
HK109_10_06	L-Y	82	10508	73086	6.88	0.07701	2.68	0.00270	3.49	0.02875	3.97	0.81	0.000832	3.45	17.4	0.6	16.8	0.6
HK109_10_07	L-Y	76	8288	65151	7.85	0.07481	2.85	0.00275	4.41	0.02854	4.76	0.83	0.000837	4.23	17.7	0.8	16.9	0.7
HK117A																		
HK117A_1_2	H-Y	101	10140	94300	9.4	0.0635	1.89	0.00244	1.80	0.02163	2.40	0.53	0.000747	1.74	15.7	0.3	15.1	0.3
HK117A_1_4	H-Y	95	10100	88700	8.8	0.0625	1.76	0.00245	1.47	0.021	2.38	0.63	0.000751	1.46	15.7	0.2	15.2	0.2
HK117A_1_6	L-Y	89	8370	83300	9.9	0.0624	1.92	0.00246	1.75	0.02111	2.79	0.67	0.000745	1.61	15.8	0.3	15.1	0.3
HK117A_1_8	L-Y	89	8050	82300	10.2	0.0642	2.02	0.00249	1.57	0.02239	2.72	0.52	0.000761	1.71	16.1	0.3	15.4	0.3
HK117A_1_9	H-Y	89	10440	87400	8.3	0.0625	1.92	0.00236	1.66	0.02028	2.51	0.60	0.000717	1.67	15.2	0.3	14.5	0.3
HK117A_1_10	L-Y	86	7850	84100	10.5	0.0637	1.88	0.00247	1.74	0.02169	2.54	0.61	0.000739	1.62	15.9	0.3	14.9	0.3
HK117A_1_11	L-Y	77	6780	71100	10.4	0.0633	1.90	0.00249	1.61	0.02165	2.31	0.56	0.000767	1.56	16.0	0.3	15.5	0.2
HK117A_1_14	H-Y	87	7170	83000	11.8	0.066	2.27	0.00253	1.78	0.02284	3.02	0.62	0.000755	1.72	16.3	0.3	15.3	0.3
HK117A_1_15	H-Y	94	6920	88100	12.6	0.0637	1.88	0.0025	1.64	0.02203	2.63	0.67	0.000759	1.58	16.1	0.3	15.3	0.2
HK117A_2_1	H-Y,R	66	10380	68600	6.6	0.0605	1.82	0.00225	1.74	0.01861	2.36	0.60	0.000702	1.85	14.5	0.3	14.2	0.3
HK117A_2_2	H-Y,R	72	7920	69800	8.8	0.0636	2.20	0.00239	1.38	0.02106	2.52	0.41	0.000743	1.62	15.4	0.2	15.0	0.2
HK117A_2_5	H-Y,R	111	8730	105400	12.1	0.0648	1.70	0.00252	1.67	0.02248	2.40	0.63	0.000761	1.71	16.2	0.3	15.4	0.3
HK117A_2_6	H-Y,R	109	7840	102700	13.2	0.0721	1.66	0.00256	1.84	0.02527	2.22	0.56	0.00077	1.82	16.5	0.3	15.6	0.3
HK117A_2_7	H-Y,R	115	8000	104400	13.2	0.1053	2.56	0.00266	1.69	0.0384	3.13	0.58	0.000781	1.79	17.1	0.3	15.8	0.3
HK117A_2_9	L-Y,C	90	6200	81800	13.3	0.0837	2.75	0.00263	1.90	0.0302	3.31	0.51	0.000796	1.88	16.9	0.3	16.1	0.3
HK117A_2_11	L-Y,C	80	6350	73900	11.7	0.0649	2.31	0.0025	1.72	0.02256	2.97	0.49	0.000776	1.80	16.1	0.3	15.7	0.3
HK117A_2_12	L-Y,C	74	8510	71800	8.5	0.0634	2.05	0.00237	1.52	0.02089	2.73	0.66	0.000746	1.47	15.2	0.2	15.1	0.2
HK117A_2_14	L-Y,C	85	6880	80600	11.7	0.0655	2.29	0.00248	1.61	0.0226	3.05	0.56	0.000772	1.55	16.0	0.3	15.6	0.3
HK117A_2_17	L-Y,C	100	7930	95700	12.0	0.0677	2.22	0.00242	1.69	0.02301	3.17	0.57	0.000768	1.69	15.6	0.3	15.5	0.3
HK117A_2_18	L-Y,C	95	8330	90700	10.8	0.0668	2.25	0.00243	1.57	0.02229	2.96	0.53	0.000782	1.53	15.6	0.3	15.8	0.2
HK117A_2_19	L-Y,C	82	8390	77300	9.1	0.104	1.73	0.00251	1.87	0.03584	2.51	0.66	0.00079	1.77	16.2	0.3	16.0	0.3
HK117A_2_20	L-Y,C	122	11690	113700	9.7	0.068	2.35	0.00236	1.91	0.02235	3.49	0.60	0.000771	1.95	15.2	0.3	15.6	0.3
HK117A_4_1	L-Y,C	154	9430	140300	14.9	0.0613	4.40	0.00239	1.76	0.02001	4.80	0.24	0.000765	1.83	15.4	0.3	15.5	0.3
HK117A_4_2	L-Y,C	146	8900	132500	15.0	0.1352	5.47	0.0026	1.69	0.0476	6.51	0.63	0.000774	1.42	16.7	0.3	15.6	0.2
HK117A_4_4	L-Y,C	154	9600	145100	15.2	0.0527	2.09	0.00231	1.34	0.01679	2.62	0.33	0.00076	1.30	14.9	0.2	15.4	0.2
HK117A_4_5	L-Y,C	147	9350	139500	15.0	0.0527	2.66	0.00231	1.21	0.01667	2.76	0.17	0.000746	1.29	14.9	0.2	15.1	0.2
HK117A_4_8	L-Y,C	119	8570	114900	13.4	0.058	2.41	0.00234	1.33	0.01883	2.66	0.31	0.000751	1.33	15.0	0.2	15.2	0.2
HK117A_4_9	L-Y,C	115	8730	110700	12.8	0.063	1.90	0.00235	1.36	0.02031	2.36	0.56	0.000753	1.46	15.2	0.2	15.2	0.2
HK117A_4_12	L-Y,C	113	14490	108300	7.5	0.0849	5.42	0.00245	1.39	0.0289	6.23	0.56	0.00076	1.45	15.8	0.2	15.4	0.2

Analysis	Position	Pb	U	Th	Th/U	$^{207}\text{Pb}/^{206}\text{Pb}$	2σ	$^{206}\text{Pb}/^{238}\text{U}$	2σ	$^{207}\text{Pb}/^{235}\text{U}^b$	2σ	Rho ^c	$^{208}\text{Pb}/^{232}\text{Th}$	2σ	$^{206}\text{Pb}/^{238}\text{U}$	2σ	$^{208}\text{Pb}/^{232}\text{Th}$	2σ
		(ppm) ^a	(ppm) ^a	(ppm) ^a		(%)		(%)		(%)		(%)		(%)	(Ma) ^d	abs	(Ma) ^e	abs
HK117A_4_13	L-Y,C	139	10750	131700	12.3	0.0544	2.02	0.00244	1.31	0.01849	2.16	0.41	0.000749	1.47	15.7	0.2	15.1	0.2
HK117A_4_14	L-Y,C	130	13100	125400	9.6	0.06393	1.42	0.00241	1.33	0.02144	2.10	0.65	0.000742	1.35	15.5	0.2	15.0	0.2
HK117A_4_15	L-Y,C	133	12510	127200	10.2	0.0612	1.80	0.00242	1.36	0.0205	2.34	0.57	0.000746	1.34	15.6	0.2	15.1	0.2
HK117A_6_1	H-Y,R	69	20490	79800	4.0	0.05789	1.59	0.00194	1.39	0.01563	2.11	0.53	0.000611	1.46	12.5	0.2	12.4	0.2
HK117A_6_2	H-Y,R	76	20060	86500	4.4	0.0599	2.00	0.00199	1.31	0.01649	2.49	0.35	0.000627	1.36	12.8	0.2	12.7	0.2
HK117A_6_3	H-Y,R	82	19660	87500	4.5	0.0613	1.63	0.00209	1.39	0.01769	2.15	0.55	0.000662	1.51	13.5	0.2	13.4	0.2
HK117A_6_4	H-Y,R	108	14880	101900	7.0	0.0627	2.07	0.00242	1.32	0.02116	2.41	0.41	0.000743	1.48	15.6	0.2	15.0	0.2
HK117A_6_5	H-Y,R	109	15870	103100	6.6	0.0661	2.27	0.00241	1.29	0.02233	2.96	0.35	0.000744	1.32	15.5	0.2	15.0	0.2
HK117A_6_6	L-Y,C	75	19060	82400	4.4	0.1051	2.47	0.00204	1.52	0.02943	2.85	0.48	0.000641	1.56	13.2	0.2	13.0	0.2
HK117A_6_7	H-Y,R	71	16850	75600	4.6	0.1395	2.44	0.00209	1.39	0.0398	2.51	0.59	0.00066	1.41	13.5	0.2	13.3	0.2
HK117A_6_9	L-Y,C	132	21580	129200	6.1	0.0591	1.69	0.0023	1.43	0.01892	2.27	0.44	0.000723	1.52	14.8	0.2	14.6	0.2
HK117A_6_10	L-Y,C	105	13490	98500	7.4	0.0653	1.99	0.00238	1.60	0.02134	2.39	0.52	0.000747	1.47	15.3	0.2	15.1	0.2
HK117A_7_3	H-Y,R	155	12910	154900	11.9	0.0658	1.82	0.00226	1.37	0.02055	2.29	0.58	0.000709	1.41	14.5	0.2	14.3	0.2
HK117A_7_4	H-Y,R	225	15220	220200	14.3	0.0578	1.45	0.00238	1.34	0.01906	1.99	0.43	0.000732	1.22	15.4	0.2	14.8	0.2
HK117A_7_5	H-Y,R	140	9000	140600	15.4	0.069	2.46	0.00231	1.73	0.02197	2.64	0.42	0.000711	1.69	14.9	0.3	14.4	0.3
HK117A_7_6	L-Y,C	105	12870	124100	9.5	0.0813	2.46	0.0019	1.84	0.02151	2.65	0.52	0.000617	1.94	12.3	0.2	12.5	0.3
HK117A_7_7	L-Y,C	114	9370	98800	10.5	0.262	1.49	0.00293	2.12	0.1059	2.64	0.82	0.00083	2.05	18.9	0.4	16.8	0.3
HK117A_7_8	L-Y,C	179	12040	176400	14.6	0.0596	1.85	0.00237	1.69	0.01928	2.54	0.68	0.000725	1.52	15.3	0.3	14.7	0.2
HK117A_7_9	L-Y,C	164	11300	155500	13.7	0.2	3.50	0.00271	1.96	0.0752	4.92	0.86	0.000761	1.58	17.5	0.3	15.4	0.3
HK117A_7_10	L-Y,C	121	9780	126400	12.9	0.0668	2.25	0.00213	1.60	0.01952	2.72	0.39	0.000683	1.61	13.7	0.2	13.8	0.2
HK117A_9_1	H-Y,R	75	2790	16100	5.7	0.6544	0.76	0.01054	2.28	0.951	2.52	0.97	0.00351	3.70	67.6	1.5	70.8	2.5
HK117A_9_3	H-Y,R	44	4590	31500	6.9	0.298	1.58	0.00302	2.81	0.1237	2.75	0.82	0.001015	3.05	19.5	0.5	20.5	0.6
HK117A_9_4	H-Y,R	20	901	4290	4.8	0.5802	1.55	0.00847	4.84	0.677	5.61	0.95	0.0034	6.47	54.4	2.7	68.6	4.4
HK117A_9_6	H-Y,R	122	10470	118400	11.4	0.0608	1.97	0.00237	1.31	0.01989	2.51	0.50	0.000731	1.35	15.3	0.2	14.8	0.2
HK117A_9_7	L-Y,C	122	10360	113100	11.0	0.0604	1.82	0.00243	1.69	0.02015	2.73	0.65	0.000758	1.58	15.7	0.3	15.3	0.2
HK117A_9_8	L-Y,C	114	9950	105400	10.6	0.0631	2.06	0.00244	1.56	0.02123	2.64	0.62	0.000762	1.57	15.7	0.3	15.4	0.2
HK117A_9_9	L-Y,C	116	10470	108800	10.5	0.0629	1.75	0.00242	1.45	0.02102	2.09	0.44	0.000748	1.60	15.6	0.2	15.1	0.2
HK117A_9_10	L-Y,C	117	10530	108200	10.3	0.0624	1.60	0.00246	1.63	0.02154	2.46	0.65	0.000754	1.72	15.8	0.3	15.2	0.3
HK117A_9_11	L-Y,C	104	10470	97400	9.3	0.0633	1.90	0.00242	1.69	0.02089	2.35	0.58	0.000742	1.62	15.6	0.3	15.0	0.3
HK117A_9_12	L-Y,C	117	11150	108900	9.8	0.0651	1.84	0.00251	1.71	0.02243	2.32	0.61	0.000763	1.57	16.2	0.3	15.4	0.2

Analysis column sample numbers refer to: SAMPLE_GRAIN_SPOT. H-Y,M-Y,L-Y refer to high, medium, and low yttrium, respectively. C and R indicate core and rim, respectively.

^aconcentration data are normalized to the primary reference material and are accurate to ~10%

^b207Pb/235U calculated assuming a natural 235U/238U ratio of 137.88

^cRho value is calculated following the method outlined in Paton et al. (2010)

^dAge calculations based on the decay constants of Jaffey et al. (1971)

^eAge calculations based on the decay constant of Amelin & Zaitsev (2002)

REFERENCES

- Amelin, Y. and Zaitsev, A., 2002, Precise geochronology of phoscorites and carbonatites: the critical role of U-series disequilibrium in age interpretations: *Geochimica et Cosmochimica Acta*, v. 66, p. 2399–2419.
- Jaffey, A.H., Flynn, K.F., Glendenin, L.E., Bentley, W.C., and Essling, A.M. 1971, Precision measurement of half-lives and specific activities of ^{235}U and ^{238}U : *Physical Review*, v. 4, p. 1889–1906.
- Paton, C., Woodhead, J., Hellstrom, J., Hergt, J., Greig, A., and Maas, R., 2010, Improved laser ablation U–Pb zircon geochronology through robust downhole fractionation correction: *Geochemistry, Geophysics and Geosystems*, v. 11, p. Q0AA06, doi:10.1029/2009GC002618.

Supplemental Information 4 (SI4)

$^{40}\text{Ar}/^{39}\text{Ar}$ thermochronology methodology

$^{40}\text{Ar}/^{39}\text{Ar}$ thermochronology was performed on muscovite grains using the following methodology. Mineral separates were obtained through standard crushing and sieving techniques and muscovites were hand-picked under a binocular microscope. Only grains with good clarity, greater than or equal to 500 μm in diameter, and void of inclusions and intergrowth were selected for thermochronology.

The $^{40}\text{Ar}/^{39}\text{Ar}$ thermochronology was performed at Queen's University Argon Geochronology laboratory. Muscovite separates and standards (used to monitor flux) were packaged in Al-foil, loaded into an 8.5 cm long and 2.0 cm diameter irradiation capsule and irradiated with fast neutrons in position 5C for a duration of 5 hours at 3 MWh at the McMaster Nuclear Reactor (Hamilton, Ontario). Packets of flux monitors were located at ~ 1 cm intervals along the irradiation container and J-values for individual samples were determined by second-order polynomial interpolation between replicate analyses of splits for each monitor position in the capsule. Typically, J-values vary by $< 10\%$ over the length of the capsule. No attempt was made to monitor horizontal flux gradients as these are considered to be minor in the core of the reactor.

Analyses were performed on samples in two separate irradiations. For each analytical session, a CO₂ laser system was used for total fusion of monitors and step-heating of samples. Between 4 and 15 irradiated muscovite grains per sample were loaded into pits of a copper sample-holder, which was then mounted beneath a ZnS view-port of a small, stainless-steel chamber connected to an ultra-high vacuum purification system. For step-heating in the first analytical session, the laser beam of a 30W New Wave Research MIR 10-30 CO₂ laser was defocused to 2 mm to cover the entire sample. For step-heating in the second analytical session, the laser beam of an identical laser was equipped with a faceted lens to allow for uniform heating of the entire sample. Heating periods were ~ 3 -4 minutes at increasing percent power settings. The evolved gas, after purification using an SAES C50 getter (~ 5 minutes), was admitted to an on-line, MAP 216 mass spectrometer, with a Bäur Signer source and an electron multiplier (set to a gain of 100 over the Faraday). Blanks, measured routinely, were subtracted from the subsequent sample gas-fractions. The extraction blanks are typically $< 10 \times 10^{-13}$, $< 0.5 \times 10^{-13}$, $< 0.5 \times 10^{-13}$, and $< 0.5 \times 10^{-13} \text{ cm}^{-3}$ STP for masses ^{40}Ar , ^{39}Ar , ^{37}Ar , and ^{36}Ar , respectively.

Measured argon-isotope peak heights were extrapolated to zero-time, normalized to the $^{40}\text{Ar}/^{36}\text{Ar}$ atmospheric ratio (295.5) using measured values of atmospheric argon, and corrected for neutron-induced ^{40}Ar from potassium, ^{39}Ar and ^{36}Ar from calcium, and ^{36}Ar from chlorine (Roddick, 1983). Dates and errors were calculated using ISOPLOT 3.75 (Ludwig, 2012), and the constants of Steiger and Jäger (1977). Uncertainties shown in the tables and on the age plateau diagrams represent the analytical precision at 2σ , assuming that the uncertainties in the ages of the flux monitors are zero. This is suitable for comparing within-spectrum variation and determining which steps form a plateau (e.g., McDougall and Harrison, 1988, p, 89). A conservative estimate of this error in the J-value is 0.5% and can be added for inter-sample comparison. The dates and J-values for the intralaboratory standard (MAC-83 biotite at 24.36 Ma; Sandeman et al., 1999) are referenced to FCT sanidine at 28.02 Ma (Renne et al., 1998) for the first analytical session, and TCR sanidine at 28.34 Ma for the second analytical session. Sample KH35 was used as an internal standard in both analytical sessions, and yielded near identical ages.

Results of the $^{40}\text{Ar}/^{39}\text{Ar}$ thermochronology are divided into well- and moderately-defined plateaus. Well-defined and moderately-defined plateaus comprise a minimum of three consecutive steps with ages of overlapping error, releasing greater than 90%, or greater than 40%, of the total ^{39}Ar , respectively.

REFERENCES

- Ludwig, K. 2012, User's manual for Isoplot v.3.75: a geochronological toolkit for Microsoft Excel, Berkeley, CA: Berkely Geochronology Center Special Publication, v. 5: revised January 30, 2012, 75p.
- McDougall, I., and Harrison, T.M., 1988, Geochronology and thermochronology by the $^{40}\text{Ar}/^{39}\text{Ar}$ Method: Oxfordshire, Oxford University Press, 212 p.
- Renne, P.R., Swisher, C.C., Deino, A.L., Karner, D.B., Owens, T.L., and DePaolo, D.J., 1998, Intercalibration of standards, absolute ages and uncertainties in $^{40}\text{Ar}/^{39}\text{Ar}$ dating: Chemical Geology, v. 145, p. 117-152, doi:10.1016/S0009-2541(97)00159-9.
- Roddick, J.C. 1983, High precision intercalibration of $^{40}\text{Ar}/^{39}\text{Ar}$ standards: Geochimica et Cosmochimica Acta, v.47, p. 887-898.
- Sandeman, H.A., Archibald, D.A., Grant, J.W., Villeneuve, M.E., and Ford, F.D., 1999, Characterization of the chemical composition and $^{40}\text{Ar}-^{39}\text{Ar}$ systematics of the interlaboratory standard MAC-83 biotite in Age and isotopic studies, Report 12, Geological Survey of Canada, Current Research 1999-F, p. 13-26.
- Steiger, R.H. and Jäger, E., 1977, Subcommission on geochronology: Convention on the use of decay constants in geo- and cosmo-chronology: Earth and Planetary Science Letters, v. 36, p. 359-362, doi:10.1016/0012-821X(77)90060-7.

Supplemental Information 5 (SI5):

$^{40}\text{Ar}/^{39}\text{Ar}$ thermochronology results

